Int J Ind Chem (2016) 7:449–456
DOI 10.1007/s40090-016-0081-0

RESEARCH

Chemical, structural and energy properties of hydrochars from microwave-assisted hydrothermal carbonization of glucose

Sunday E. Elaigwu[1,2] · **Gillian M. Greenway**[1]

Received: 20 November 2015 / Accepted: 15 April 2016 / Published online: 9 May 2016

Abstract Hydrothermal carbonization has been used as a green and effective technique for the preparation of hydrochars from simple carbohydrates, such as glucose. The chemical and structural properties of hydrochars prepared from glucose have been studied. However, the energy properties of hydrochars prepared from microwave-assisted hydrothermal carbonization of glucose have not been studied. Thus, in this study, microwave-assisted hydrothermal carbonization of glucose, and the energy properties of the prepared hydrochars are reported. The preparation involved heating glucose in de-ionized water at 200 °C for 5–60 min in a microwave oven. The prepared hydrochars were characterized using scanning electron microscope, nitrogen sorption measurement, Fourier transform infrared spectroscopy, elemental (CHN) analyzer, and nuclear magnetic resonance, and their energy properties studied. The result indicated that, in comparison with previous studies using the classical hydrothermal carbonization process, this approach reduced the processing time greatly from hours to 45 min, while the increase in higher heating value of the hydrochar when compared to that of the starting material was higher in this study than some value previously reported.

Keywords Microwave · Hydrothermal · Carbonization · Glucose · Energy properties · Hydrochar

Introduction

The use of cheap, fast and different environmentally friendly strategies for the preparation of carbon materials from renewable resources has been on the increase in recent times in the areas of environmental science and technology. This is because of the vital roles these materials play in different applications, such as adsorbents, catalyst supports, energy storage materials, electrode materials, and stationary phases in liquid chromatography [1, 2]. As a result, a number of approaches such as pyrolysis, arc discharge, chemical vapor decomposition, and hydrothermal treatment have been used in the preparation of these carbon materials [3]. Hydrothermal carbonization is a process of decomposing an organic material in hot water under high pressure to produce solid carbon material (hydrochar) and water soluble organics. It is a green and efficient approach for treating organic materials because of its comparatively low emission, and generation of non-toxic waste [4]. Due to its simple operation, mild reaction conditions, and ability to exploit renewable biomass with minimal pre-treatment, it is of a particular environmental advantage when compared to other techniques of carbonization [5–7]. Among potential precursors used in the preparation of carbonaceous materials, glucose is very promising and its hydrothermal carbonization process has been studied several times using the conventional method of oven heating [6, 8–10]. However, the conventional hydrothermal process requires special systems that support pressure and temperature, usually an autoclave with pressure safety device is used. Also, the reaction times are

Electronic supplementary material The online version of this article (doi:10.1007/s40090-016-0081-0) contains supplementary material, which is available to authorized users.

✉ Sunday E. Elaigwu
S.E.Elaigwu@2009.hull.ac.uk; sunnietrinex@hotmail.com

[1] Department of Chemistry, University of Hull, Cottingham Road, Hull HU6 7RX, UK

[2] Department of Chemistry, University of Ilorin, PMB 1515, Ilorin, Kwara, Nigeria

usually in hours, which makes the process expensive and time consuming.

In many applications, the use of microwave heating as an attractive alternative to conventional method of heating has shown to be more energy efficient, because it provides selective, fast and homogenous heating, which reduces processing time and costs significantly [11, 12]. It has also been established that irradiation with microwave produced effective internal heating by direct coupling of microwave energy with solvents, reagents and catalysts, which increased the reactions greatly [13]. The use of microwave heating in hydrothermal carbonization process, and in the preparation of hydrochar from biomasses, glucose and other materials, such as human waste, cellulose and starch, has been reported [4, 14–19]. Some of these processes usually proceed via the degradation of starch or cellulose to form glucose and then further carbonization of the formed glucose. However, the energy properties of hydrochars obtained using glucose as starting material have not been previously reported to the best of our knowledge. Therefore, in this study the energy properties of hydrochars from microwave-assisted hydrothermal carbonization process using glucose as starting material are reported.

Materials and methods

Anhydrous D-glucose was purchased from Fisher Scientific, UK and was used throughout without further purification.

Microwave-assisted hydrothermal carbonization of glucose

5 g each of glucose was dissolved in 5 mL of de-ionized water in 100 ml microwave reaction vessels made of Teflon to form supersaturated solutions. The vessels were sealed and placed in a 2.45 GHz magnetron frequency microwave oven (MARS, CEM, Milton Keynes, UK equipped with XP1500 digestion vessels, and 1600 W at maximum power), and were hydrothermally carbonized at 200 °C in the microwave oven which was set to ramp to a given temperature in 5 min, and then held at the temperature for 5–60 min. The reaction system was allowed to cool to room temperature, and the carbonized materials were filtered off using Whatman filter paper number 3, ashless 11 cm. The solid chars (hydrochars) obtained were washed gently with de-ionized water to remove any left over of the liquid phase of the reaction, and were dried in a conventional oven at 80 °C for 16 h.

Mass yield

In each case, the dry mass of the carbonized material was measured and the mass yield (dry mass percentage of starting material) was calculated as follows:

$$\text{Mass yield } (\%) = \frac{\text{Mass of carbonized material (g)}}{\text{Mass of starting material (g)}} \times 100. \quad (1)$$

Energy properties of the hydrochars

In place of a calorimeter to experimentally determine the energy content, the higher heating value (HHV) was calculated using Eq. 2 (Dulong equation) as previously reported [20]. This formula is one of the first correlations to estimate the HHV of coals, which is still in used by many researchers today and has also been applied to oils [21].

$$\text{HHV} = 0.3383\text{C} + 1.422(\text{H} - 0/8). \quad (2)$$

The energy densification ratios of the hydrochars were calculated using the following equation:

$$\text{Energy densification ratio} = \frac{\text{HHV of dried hydrochar}}{\text{HHV of dried starting material}}. \quad (3)$$

All experiments were carried out in triplicate, and the results obtained are presented in Table 1.

Characterization techniques

The prepared hydrochars were characterized using the following instruments: Fisons instruments EA 1108 CHN analyser (Fison Instrument, Crawley, UK) was used for CHN analysis; samples were ground into fine powder, weighed into tin capsules and placed on the autosampler for analysis. Surface area and pore size distribution were measured using a Micromeritics Tristar BET-N_2 surface area analyser (Micromeritics, Hexton, UK). Before the analysis, samples were degassed under nitrogen atmosphere at 120 °C for 3 h. FT-IR spectra were recorded on Thermo Scientific Nicolet 380 FT-IR (Themo Scientific, Hemel Hempstead, UK), equipped with attenuated total reflectance (ATR). The samples were in direct contact with ATR diamond crystal, and each sample was investigated in wavenumber range of 4000–525 cm^{-1} using 16 scans at a spectral resolution wavenumber of 4 cm^{-1}. The morphologies and particle sizes were visualized with a ZEISS EVO 60 SEM (Carl Zeiss, Cambridge, UK); samples were coated with gold and platinum alloy and impregnated on a sticky disc before analysis. ^{13}C solid state magic angle

Table 1 Elemental composition, mass yield, O/C and H/C atomic ratios, and energy properties of glucose and hydrochars, with data from previous studies using the conventional approach for comparison

Temperature and time	C (%)	H (%)	N (%)	O (%)[a]	Mass yield (%)	O/C[b]	H/C[b]	HHV (MJ/kg)	Energy densification ratio	Energy yield (%)
Glucose	39.84 ± 0.06	6.84 ± 0.09	0.00	53.32 ± 0.15	–	1.00	2.04	13.73	–	–
200 °C for 60 min	61.98 ± 0.56	4.43 ± 0.22	0.00	33.59 ± 0.32	37.28 ± 1.16	0.41	0.85	21.30	1.55	57.84
200 °C for 45 min	62.32 ± 1.80	4.31 ± 0.70	0.00	33.37 ± 1.10	40.03 ± 0.98	0.40	0.82	21.30	1.55	62.06
200 °C for 30 min	60.66 ± 2.15	4.64 ± 1.58	0.00	34.70 ± 0.57	32.67 ± 1.23	0.43	0.91	20.95	1.53	49.87
200 °C for 20 min	58.64 ± 0.60	4.90 ± 0.55	0.00	36.46 ± 1.15	25.01 ± 0.56	0.47	1.00	20.33	1.48	37.03
200 °C for 15 min	52.81 ± 0.12	4.61 ± 0.10	0.00	42.58 ± 0.02	20.69 ± 1.48	0.61	1.04	16.85	1.23	25.40
Glucose (210 °C for 4.5 h) [9]	66.29	4.15	–	29.56	28.00	0.334	0.752	–	–	–
Prosopis africana shell (200 °C for 4 h) [24]	57.86	6.37	1.46	34.31	30.85	0.44	1.31	22.53	1.28	–
Anaerobically digested maize silage (190 °C for 10 h) [25]	62.13	6.87	–	27.44	65.0	0.33	1.33	27.0	–	–

[a] Oxygen content was determined by difference [100 % − (C % + H % + N %)]

[b] Atomic ratios

spinning NMR experiment was carried out on a Bruker Avance II 500 MHz (11.74T) spectrometer (Bruker, Coventry, UK); samples were packed without further treatment into a 4 mm zirconia rotor sample holder spinning at MAS rate $\nu_{MAS} = 8$ kHz. Carbon sensitivity was enhanced by Proton-to-carbon CP MAS: recycle delay for all CP experiments was 3 s and TPPM decoupling was used during signal acquisition. Cross polarization transfer was carried out under adiabatic tangential ramps to enhance the signal with respect to other known methods. CP time $t_{CP} = 500$ ms. The number of transients for all carbon samples was 200.

Results and discussion

Effect of time on the microwave-assisted hydrothermal carbonization of glucose

The effect of time on the process is presented in Table 1. As the processing time was increased from 15 to 60 min, different mass yields were obtained for the hydrochars. The mass yield increased between 15 and 45 min, and decreased afterwards. Hence, processing time above 60 min was not considered. Maximum mass yield for the hydrothermal carbonization of glucose has been reported to be obtained at 200 °C [6], while further increase in temperature will lead to a gradual decrease in mass yield; reason being that increase in temperature favors gasification reactions, which results in part of the hydrothermal carbon being lost in form of volatile compounds [22, 23]. Hence, temperatures above 200 °C were not considered in this study. Falco et al. [6], using conventional hydrothermal carbonization process, reported a maximum mass yield of about 40 % for glucose hydrochar at 200 °C for 24 h, which is consistent with the maximum mass yield obtained in this study under microwave heating, despite the shorter time (45 min) in the microwave oven.

Elemental composition of the prepared hydrochars

The elemental compositions (C, O, and H) of the starting material (glucose) and different hydrochar samples are listed in Table 1. It was observed that carbon contents increased from 39.84 % in the starting material to about 53–62 % in the hydrochar samples. The oxygen and hydrogen contents of the hydrochars reduced at the same time. These variations, which increased with reaction time, are consistent with hydrothermal carbonization processes. The gradual increase in carbon content, and the decrease in hydrogen and oxygen contents of the hydrochars, with increase in processing time is due to loss of hydrogen and oxygen in deoxygenating, dehydration and decarboxylation reactions that occurred during the microwave-assisted hydrothermal carbonization process [6, 22, 26, 27]. Despite the shorter time used in this study under microwave heating, the result is similar to previous studies [6, 9].

The changes in elemental compositions were further analyzed using the van Krevelen diagram (Fig. 1), by plotting the atomic H/C against the atomic O/C. The diagram provided further evidence about the transformation (dehydration, decarboxylation, and demethanation

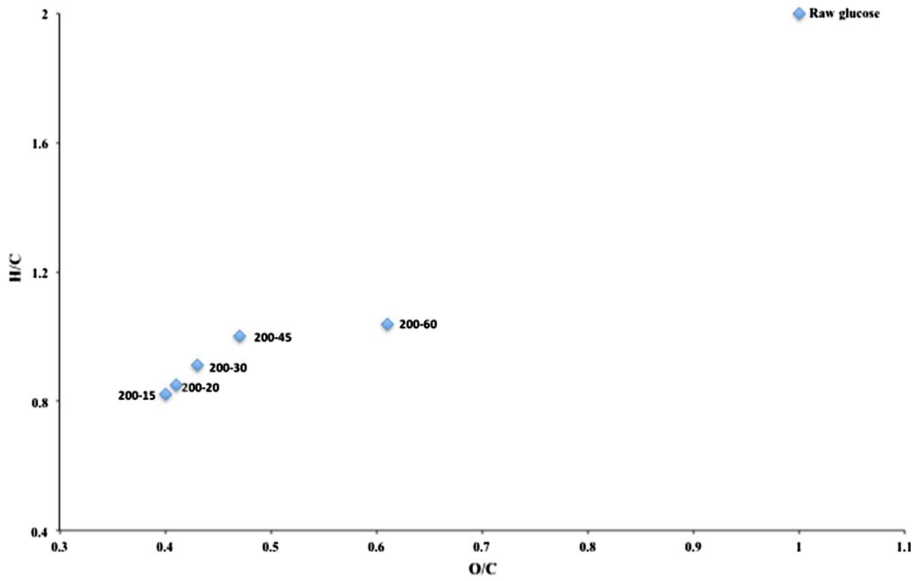

Fig. 1 van Krevelen diagram of raw glucose and hydrochars prepared at 200 °C and different processing time

reactions) that took place in the chemical structure of glucose during the microwave-assisted hydrothermal carbonization process. The transformation from the starting material (glucose) to the hydrochar samples follows a diagonal line due to decrease in the O/C and H/C ratios, suggesting dehydration reactions as prevalent reaction during the process, which is consistent with previous reports [9, 28].

Energy properties of the prepared hydrochars

An important parameter to test the quality of hydrochars is their higher heating value (HHV). It provides information about the quantity of energy present in the hydrochar. The calculated HHV increased with increase in residence time from 16.90 MJ/kg in 15 min to 21.30 MJ/kg in 45 min, and remained stable afterwards (Table 1). This increase in higher heating value of the hydrochars with increase in processing time is consistent with previous report [29]. The highest HHV in this study showed an increase of 55.5 % when compared to that of the starting material, against 39 % previously reported for loblolly pine [29], 45.20 % for bamboo [30], and 21 % for dry leaves [31].

As stated earlier, dehydration, decarboxylation, and condensation reactions are associated with hydrothermal carbonization process. This leads to the carbonization of the starting material and consequently results in energy densification, which is used to measure the effectiveness of the hydrothermal carbonization processes [32, 33]. In this study, energy densification ratios of the hydrochars (Table 1) increased with increase in reaction time and ranged from 1.23 to 1.55, which is consistent with previous reports [29, 31].

The energy yield is defined as the mass yield of the hydrochar multiply by its energy densification ratio. The result of the energy yield for the hydrochars is presented in Table 1. The lowest energy yield of 25.40 % was obtained when the reaction time was 15 min, and increased steadily until the maximum hydrochar energy yield of 62.06 % was obtained after 45 min. Thus, the hydrochar prepared at 200 °C for 45 min has the highest mass yield, HHV, energy densification, and energy yield. Therefore, further characterization will be focused on this hydrochar.

FT-IR analysis

The FT-IR spectra (Fig. 2) gave further insight into changes in the chemical composition of glucose during the process. Comparing the FT-IR results of glucose (Fig. 2a) and that of the hydrochar prepared at 200 °C for 45 min (Fig. 2b) indicates that dehydration and aromatization of glucose occurred during the process. The allocation of the functional groups was based on previous reports [9, 34]. The broad peak between 3600 and 3000 cm^{-1} (section 1) corresponds to stretching vibration of aliphatic O–H (hydroxyl and carboxyl), while the peaks between 1500 and 1000 cm^{-1} (section 5) correspond to C–O stretching vibration from esters, ether, phenols, and aliphatic alcohols. The weak intensity of these peaks (sections 1 and 5) is an indication that dehydration and decarboxylation reactions occurred during the process. The peaks between 1800 and 1650 cm^{-1} (section 3) present only in the hydrochar result from C=O vibration of esters, quinone, pyrone, carboxylic acids or aldehydes, while the appearance of peaks between 1650 and 1500 cm^{-1} (section 4) due to C=C vibrations, and well-

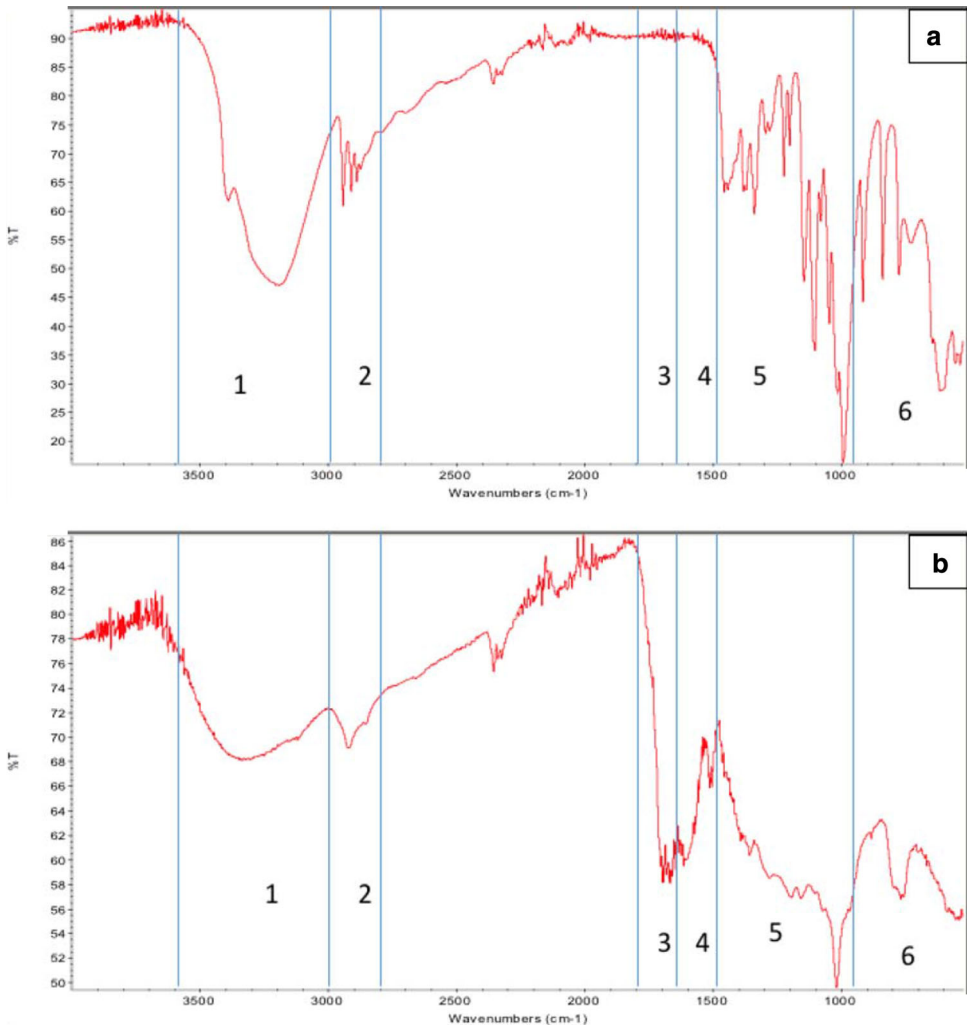

Fig. 2 FT-IR spectra of **a** glucose, **b** hydrochar prepared at 200 °C 45 min

defined peak below 1000 cm^{-1} (section 6) from deformation of C–H out of plane bending vibrations in aromatic compounds, showed the aromatic nature of the hydrochar. The peaks between 3000 and 2800 cm^{-1} (section 2) due to stretching vibration of aliphatic C–H bonds, indicate the presence of aliphatic structures.

NMR analysis

^{13}C solid state NMR analysis is usually used as a complementary technique to FT-IR analysis in describing the level of conversion during hydrothermal carbonization process [24]. The ^{13}C solid state NMR spectrum of the hydrochar prepared at 200 °C for 45 min shown in Fig. S1 (Supplementary information) provided information about its chemical composition, and also confirmed the results from the FT-IR. The peaks between 14 and 60 ppm are due to the presence of aliphatic carbons [8, 35], while those between 100 and 160 ppm usually referred to as the aromatic region are all due to C=C bond, but between 140 and 160 ppm are specifically due to the oxygen bound O–C=C (O-aryl) [35]. The peaks between 170 and 200 ppm are due to the presence of carboxylic acid, aldehydes or ketones moieties [36]. The spectrum also shows carbohydrate resonances (specifically CH_2OH groups around 62 ppm, CHOH groups around 72 ppm, and anomeric O–C–O carbons around 90 ppm) in the O-alkyl region between 60 and 100 ppm [37, 38]. These functional groups have already been indicated by the FT-IR result. Thus, both results are in good agreement with each other, and clearly show the formation of the hydrochar structure under the microwave-assisted process.

SEM analysis

The scanning electron microscope (SEM) analysis (Fig. 3) provided information about the structural morphologies of the starting material (glucose) and the hydrochar prepared at 200 °C for 45 min. The morphological features of

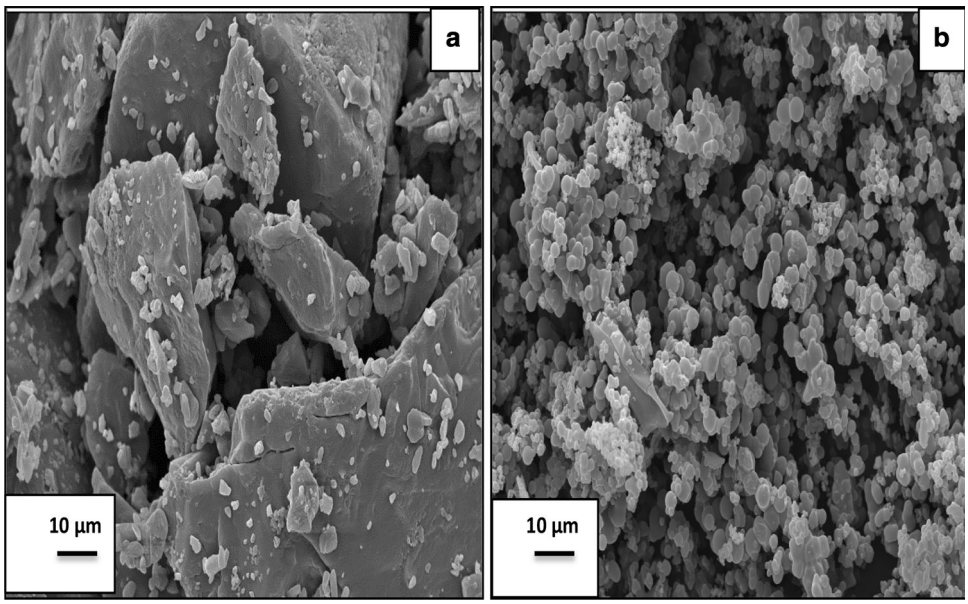

Fig. 3 SEM images of **a** glucose, **b** hydrochar prepared at 200 °C 45 min

glucose (Fig. 3a) as visualized are completely different from those of the hydrochar (Fig. 3b). The sphere-like microparticles of different sizes (1–10 µm) seen on the SEM image of the hydrochar are in contrast to the block of materials observed in glucose. The mechanism in which these microparticles are generated is based on hydrolysis, dehydration and polymerization of glucose as stated in the mechanism, while the spherical nuclei are formed to minimize the energy of the interface [6, 14].

Surface area analysis

The hydrochar prepared at 200 °C for 45 min showed a Type II isotherm based on the IUPAC system of classification from the nitrogen sorption measurement in Fig. S2 (Supplementary information). This is a typical isotherm obtained with non-porous materials. It is, therefore, not surprising that the hydrochar has a very small BET surface area of 3.3 ± 0.7 m^2g^{-1}, due to poor porosity. The hydrothermal carbonization process involves carbonization and solubilization of organics leading to the formation of tarry substances, which usually contaminate the hydrochars, plugging their pores, and making the apparent BET surface area to be small [39]. Similar results have been reported using the conventional hydrothermal method [9, 40]. Thus, surface area and porosity improvement are usually carried out for the hydrochars to fit into specific applications, such as hydrogen or electrical energy storage [33].

Mechanism for the hydrochar formation

Similar mechanism to that in conventional hydrothermal carbonization process is expected to occur under the microwave-assisted process [41]. However, under the electromagnetic irradiation during the microwave-assisted process, temperature and pressure will play a very vital role by enhancing the different reactions (dehydration, polymerization and aromatization), thereby accelerating the process [12]. Therefore, in this study, glucose fragments by hydrolysis and dehydrates under microwave heating to form different soluble furfural-like compounds. The dehydration reaction is indicated in the hydrochar by the reduction in the OH peak between 3600 and 3000 cm^{-1}. The furfural-like compounds undergo further decomposition to form acids, aldehydes and phenols [18, 42], indicated in the hydrochar by the appearance of the peaks between 1800 and 1650 cm^{-1} (C=O vibration). The dehydration of water from the equatorial hydroxyl groups could be the mechanism responsible for the appearance of C=O groups [43]. The glucose and its decomposition products then undergo polymerization or condensation reactions, which could be caused by intermolecular dehydration or through aldol condensation leading to the formation of soluble polymers [9]. The aromatization of the polymers also occurs simultaneously with the formation of C=C linkages (indicated by the appearance of peaks between 1650–1500 cm^{-1}, and 100–160 ppm in the FTIR and NMR spectra of the hydrochar, respectively), which could result from keto-enol tautomerism of the dehydrated species, intermolecular dehydration or via the condensation of the aromatized molecules formed during the decomposition or dehydration of the glucose [9, 43]. A burst nucleation process occurs once the amount of aromatic clusters in aqueous phase reaches the critical super saturation point. The formed nuclei then grow through diffusion to the surface of the chemical species that are present

in solution (as seen on the SEM image of the hydrochar) to minimize the energy of the interfaces [14]. The reactive oxygen functionalities (as indicated by the FTIR and NMR spectra), such as hydroxyl, carbonyl, and carboxylic, present on the outer surface of the microspheres and in the reactive species helps to quickly link the species to the microspheres [43]. Due to this linkage, stable oxygen groups, such as ether, pyrone or quinone, usually found at the center of the resulting microsphere are formed, and as a result, when the growth process ends, the outer surface of the hydrochar particles will have a high concentration of reactive oxygen groups, while the core will have less reactive oxygen groups [9, 43]. Thus, two types of products are formed in the reaction medium at the end of the reaction, namely the insoluble solid residue (hydrochar), and the aqueous soluble organic phase (consisting of furfural-like compounds, aldehydes and acids). Thus, as the reaction time is increased in this study, it is expected that the aromatization and polymerization processes will also be favoured, which will increase the yield of the hydrochar.

Conclusion

Microwave-assisted hydrothermal carbonization was successfully used to prepare hydrochar from glucose. The chemical and structural characterization of the prepared hydrochar showed that it is similar to those previously prepared using the conventional oven method of hydrothermal carbonization. This implies that the microwave-assisted hydrothermal approach is a fast and simple approach for preparing the hydrochar as it reduced the processing time from hours to few minutes. The energy properties of the prepared hydrochars in relationship to some published results showed a higher increase in HHV of the hydrochars when compared to that of the starting material.

Acknowledgments The authors are grateful to Petroleum Technology Development Fund (PTDF), Nigeria for providing the PhD studentship for Dr. Sunday E. Elaigwu, and Bob Knight for his assistant with the CEM microwave oven.

References

1. Elaigwu SE, Greenway GM (2014) Biomass derived mesoporous carbon monoliths via an evaporation-induced self-assembly. Mater Lett 115:117–120
2. Liu S, Tian J, Wang L, Zhang Y, Qin X, Luo Y, Asiri AM, Al-Youbi AO, Sun X (2012) Hydrothermal treatment of grass: a low-cost, green route to nitrogen-doped, carbon-rich, photoluminescent polymer nanodots as an effective fluorescent sensing platform for label-free detection of Cu (II) ions. Adv Mater 24:2037–2041
3. Latham KG, Jambu G, Joseph SD, Donne SW (2014) Nitrogen doping of hydrochars produced hydrothermal treatment of sucrose in H_2O, H_2SO_4, and NaOH. ACS Sustain Chem Eng 2:755–764
4. Elaigwu SE, Rocher V, Kyriakou G, Greenway GM (2014) Removal of Pb^{2+} and Cd^{2+} from aqueous solution using chars from pyrolysis and microwave-assisted hydrothermal carbonization of *Prosopis africana* shell. J Ind Eng Chem 20:3467–3473
5. Kambo HS, Dutta A (2015) A comparative review of biochar and hydrochar in terms of production, physico-chemical properties and applications. Renew Sustain Energy Rev 45:359–378
6. Falco C, Baccile N, Titirici MM (2011) Morphological and structural differences between glucose, cellulose and lignocellulosic biomass derived hydrothermal carbons. Green Chem 13:3273–3281
7. Reza MT, Mumme J, Ebert A (2015) Characterization of hydrochar obtained from hydrothermal carbonization of wheat straw digestate. Biomass Conv Bioref. doi:10.1007/s13399-015-0163-9
8. Demir-Cakan R, Baccile N, Antonietti M, Titirici MM (2009) Carboxylate-rich carbonaceous materials via one-step hydrothermal carbonization of glucose in the presence of acrylic acid. Chem Mater 21:484–490
9. Sevilla M, Fuertes AB (2009) Chemical and structural properties of carbonaceous products obtained by hydrothermal carbonization of saccharides. Chem Eur J 15:4195–4203
10. Yao C, Shin Y, Wang LQ, Windish CF, Samuels WD, Arey BW, Wang C, Risen WM, Exarhos GJ (2007) Hydrothermal dehydration of aqueous fructose solutions in a closed system. J Phys Chem C 111:15141–15145
11. Nüchter M, Ondruschka B, Bonrath W, Gum A (2004) Microwave assisted synthesis—a critical technology overview. Green Chem 6:128–141
12. Elaigwu SE, Kyriakou G, Prior TJ, Greenway GM (2014) Microwave-assisted hydrothermal synthesis of carbon monolith via a soft-template method using resorcinol and formaldehyde as carbon precursor and pluronic F127 as template. Mater Lett 123:198–201
13. Guo F, Fang Z, Zhou TJ (2012) Conversion of fructose and glucose into 5-hydroxymethylfurfural with lignin-derived carbonaceous catalyst under microwave irradiation in dimethyl sulfoxide–ionic liquid mixtures. Bioresour Technol 112:313–318
14. Guiotoku M, Rambo CR, Hansel FA, Magalhaes WLE, Hotza D (2009) Microwave-assisted hydrothermal carbonization of lignocellulosic materials. Mater Lett 63:2707–2709
15. Guiotoku M, Rambo CR, Hotza D (2014) Charcoal produced from cellulosic raw materials by microwave-assisted hydrothermal carbonization. J Therm Anal Calorim 117:269–275
16. Afolabi OOD, Sohail M, Thomas CPL (2015) Microwave hydrothermal carbonization of human biowastes. Waste Biomass Valor 6:147–157
17. Hassanzadeh S, Aminlashgari N, Hakkarainen M (2014) Chemoselective high yield microwave assisted reaction turns cellulose to green chemicals. Carbohyd Polym 112:448–457
18. Wu D, Hakkarainen M (2014) A closed-loop process from microwave-sssisted hydrothermal degradation of starch to utilization of the obtained degradation products as starch plasticizers. ACS Sustain Chem Eng 2:2172–2181
19. Möller M, Harnisch F, Schröder U (2012) Microwave-assisted hydrothermal degradation of fructose and glucose in subcritical water. Biomass Bioenerg 39:389–398

20. Gao Y, Wang X, Wang J, Li X, Cheng J, Yang H, Chen H (2013) Effect of residence time on chemical and structural properties of hydrochar obtained by hydrothermal carbonization of water hyacinth. Energy 58:376–383
21. Kieseler S, Neubauer Y, Zobel N (2013) Ultimate and proximate correlations for estimating the higher heating value of hydrothermal solids. Energy Fuels 27:908–918
22. Berge ND, Ro KS, Mao J, Flora JRV, Chappell MA, Bae S (2011) Hydrothermal carbonization of municipal waste streams. Environ Sci Technol 45:5696–5703
23. Kruse A, Gawlik A (2003) Biomass conversion in water at 330–410 °C and 30–50 MPa. Identification of key compounds for indicating different chemical reaction pathways. Ind Eng Chem Res 42:267–279
24. Elaigwu SE, Greenway GM (2016) Microwave-assisted and conventional hydrothermal carbonization of lignocellulosic waste material: comparison of the chemical and structural properties of the hydrochars. J Anal Appl Pyrol. doi:10.1016/j.jaap.2015.12.013
25. Mumme J, Eckervogt L, Pielert J, Diakité M, Rupp F, Kern J (2011) Hydrothermal carbonization of anaerobically digested maize silage. Bioresour Technol 102:9255–9260
26. Sevilla M, Maciá-Agulló JA, Fuertes AB (2011) Hydrothermal carbonization of biomass as a route for the sequestration of CO_2: chemical and structural properties of the carbonized products. Biomass Bioenerg 35:3152–3159
27. Kang S, Li X, Fan J, Chang J (2012) Characterization of hydrochars produced by hydrothermal carbonization of lignin, cellulose, D-xylose, and wood meal. Ind Eng Chem Res 51:9023–9031
28. Erdogan E, Atila B, Mumme J, Reza MT, Toptas A, Elibol M, Yanik J (2015) Characterization of products from hydrothermal carbonization of orange pomace including anaerobic digestibility of process liquor. Bioresour Technol 196:35–42
29. Hoekman SK, Broch A, Robbins C (2011) Hydrothermal carbonization (HTC) of lignocellulosic biomass. Energy Fuels 25:1802–1810
30. Li MF, Shen Y, Sun JK, Bian J, Chen CZ, Sun RC (2015) Wet torrefaction of bamboo in hydrochloric acid solution by microwave heating. ACS Substain Chem Eng 3:2022–2029
31. Saqib NU, Oh M, Jo W, Park SK, Lee JY (2015) Conversion of dry leaves into hydrochar through hydrothermal carbonization (HTC). J Mater Cycles Waste Manag. doi:10.1007/s10163-015-0371-1
32. Xu Q, Qian Q, Quek A, Ai N, Zeng G, Wang J (2013) Hydrothermal carbonization of macroalgae and the effects of experimental parameters on the properties of hydrochars. ACS Sustain Chem Eng 1:1092–1101
33. Parshetti GK, Kent HS, Balasubramanian R (2013) Chemical, structural and combustion characteristics of carbonaceous products obtained by hydrothermal carbonization of palm empty fruit bunches. Bioresour Technol 135:683–689
34. Tekin K, Pileidis FD, Akalin MK, Karagöz S (2015) Cellulose-derived carbon spheres produced under supercritical ethanol conditions. Clean Technol Environ Policy. doi:10.1007/s10098-015-1014-x
35. Baccile N, Laurent G, Babonneau F, Fayon F, Titirici MM, Antonietti M (2009) Structural characterization of hydrothermal carbon spheres by advanced solid-state MAS C-13 NMR investigations. J Phys Chem C 113:9644–9654
36. Sun K, Ro KS, Guo M, Novak JM, Mashayekhi H, Xing B (2011) Sorption of bisphenol A, 17a-ethinyl estradiol and phenanthrene on thermally and hydrothermally produced biochars. Bioresour Technol 102:5757–5763
37. Cao X, Ro KS, Chappell M, Li Y, Mao J (2011) Chemical structures of swine-manure chars produced under different carbonization conditions investigated by advanced solid-state ^{13}C nuclear magnetic resonance (NMR) spectroscopy. Energy Fuels 25:388–397
38. Mao J, Holtman KM, Scott JT, Kadla J, Schmidt-Rohr K (2006) Differences between lignin in unprocessed wood, milled wood, mutant wood, and extracted lignin detected by ^{13}C solid-state NMR. J Agric Food Chem 54:9677–9686
39. Mochidzuki K, Sato N, Sakoda A (2005) Production and characterization of carbonaceous adsorbents from biomass wastes by aqueous phase carbonization. Adsorption 11:669–673
40. Titirici MM, Antonietti M, Baccile N (2008) Hydrothermal carbon from biomass: a comparison of the local structure from poly- to monosaccharides and pentoses/hexoses. Green Chem 10:1204–1212
41. Guiotoku M, Maia CMBF, Rambo CR, Hotza D (2011) Synthesis of carbon-based materials by microwave hydrothermal processing. In: Chandra U (ed) Microwave heating. InTech, New York
42. Kabyemela BM, Adschiri T, Malaluan RM, Arai K (1999) Glucose and fructose decomposition in subcritical and supercritical water: detailed reaction pathway, mechanisms, and kinetics. Ind Eng Chem Res 38:2888–2895
43. Sevilla M, Fuertes AB (2009) The production of carbon materials by hydrothermal carbonization of cellulose. Carbon 47:2281–2289